

272 As described in the first report by Oguchi, the intensity of the tapetal-like reflex varied
273 depending on the direction of the observation light against the retina.^{1,17} A similar
274 finding was reported for patients with X-linked retinoschisis.¹⁰ This is probably because
275 the layer where the tapetal-like reflex originates has the properties of a plane mirror, viz.,
276 the angle of reflection equals the angle of incidence. If the incident angle is almost
277 perpendicular to the retinal surface, strong tapetal-like reflex can be observed, but if it is
278 not, the intensity of the reflex decreases.¹⁷ These reflective materials can be either
279 layered structures or particles or chemical materials embedded in the outer segment
280 discs, which are well aligned structures parallel to the retinal surface. The
281 Mizuo-Nakamura phenomenon can be explained by the disappearance of mirror-like
282 reflective materials following prolonged dark-adaptation. The incident angle against the
283 reflective materials, however, can be easily changed by the interfering retinal structures
284 which have different refractive indices, such as a thickened vitreo-retinal interface or
285 vessel walls of retinal arteries or thickened RNFL. Changes in the distribution patterns
286 of the tapetal-like reflex in Figure 4 can be more easily explained by the modulation of
287 outer retinal reflex due to the inner retinal structures than by the local functional changes
288 of the photoreceptors or RPEs *per se*. The increased or decreased reflectivity of the
289 tapetal-like reflex may be due to the refractive structures which change the incident

290 angle of the observation light. For example, vitreous traction on the retina can change
291 during the natural course of the disease process, and this may change the reflection of
292 the vitreo-retinal interface, leading to the changes in distribution of the dark regions as
293 observed in some of our cases (**Fig. 2**).

294 In addition, the direction and strength of the vitreoretinal traction may change during
295 aging even before the posterior vitreous detachment is completed. This may explain
296 the spontaneous changes in the distribution patterns of the dark regions in younger
297 patients. The observations by OCT, however could not detect either non-homogeneous
298 vitreous distribution or posterior hyaloid detachment locally along the border of the dark
299 regions (**Fig.8**). The interfering materials which can decrease the tapetal-like reflex
300 may be too small and thin to be detected by the current imaging techniques.

301 The decreased or increased reflectivity along arteries could be similarly explained (**Fig.**
302 **6**). Compared to the retinal veins, the retinal arteries are composed of additional
303 muscle layers and appear more hyperreflective.¹⁸ Light passing beside the retinal
304 arteries may be refracted and change the reflectance from the outer retina, although part
305 of dark regions along the artery look too large to be simply explained by this change (**Fig.**
306 **6C**).

307 The alterations of the dark and tapetal-like reflex regions can be explained by changes

308 in the refractive modulations in the inner retina. However, we could not find any metallic
309 reflex in the dark regions even though we examined the retina from different directions
310 (data not shown). The border between regions with and without tapetal-like reflex was
311 always clear irrespective of the viewing angle. There must be another mechanism
312 which changes the retinal reflectivity in Oguchi's disease.

313 The tapetal-like reflex of the Mizuo-Nakamura phenomenon has been reported in
314 other diseases such as X-linked cone-rod dystrophy,¹⁹ X-linked retinoschisis,^{10,20} and
315 also in carriers of X-linked retinitis pigmentosa.²¹ The underlying mechanism for this
316 reflex has not been clearly determined by our case series, and the discussion we have
317 made regarding possible mechanisms is very speculative. However, our results have
318 given us important insights on the origin of this unusual fundus reflex.

319

320 **References**

321

322 1. Oguchi C. Ueber eine Abart von Hemeralopie. *Acta Soc Ophthalmol Jpn*

323 1907;11:123-134.

324 2. Mizuo G, Nakamura B. On new discovery in dark adaptation in Oguchi's disease.

325 *Acta Soc Ophthalmol Jpn* 1914;18:73-126.

326 3. Fuchs S, Nakazawa M, Maw M, Tamai M, Oguchi Y, Gal A. A homozygous 1-base

327 pair deletion in the arrestin gene is a frequent cause of Oguchi disease in Japanese.

328 *Nature genetics* 1995;10:360-362.

329 4. Yamamoto S, Sippel KC, Berson EL, Dryja TP. Defects in the rhodopsin kinase gene

330 in the Oguchi form of stationary night blindness. *Nature genetics* 1997;15:175-178.

331 5. Nakazawa M, Wada Y, Fuchs S, Gal A, Tamai M. Oguchi disease: phenotypic

332 characteristics of patients with the frequent 1147delA mutation in the arrestin gene.

333 *Retina* 1997;17:17-22.

334 6. Nakamura M, Yamamoto S, Okada M, Ito S, Tano Y, Miyake Y. Novel mutations in

335 the arrestin gene and associated clinical features in Japanese patients with Oguchi's

336 disease. *Ophthalmology* 2004;111:1410-1414.

337 7. Saga M, Mashima Y, Kudoh J, Oguchi Y, Shimizu N. Gene analysis and evaluation of

338 the single founder effect in Japanese patients with Oguchi disease. *Jpn J Ophthalmol*
339 2004;48:350-352.

340 8. Kuwabara Y, Ishihara K, Akiya S. Histopathological and Electron Microscopic
341 Studies on the Retina of Oguchi's disease. *Acta Soc Ophthalmol Jpn*
342 1963;67:1323-1351.

343 9. Yamanaka M. Histologic study of Oguchi's disease. Its relationship to pigmentary
344 degeneration of the retina. *Am J Ophthalmol* 1969;68:19-26.

345 10. de Jong PT, Zrenner E, van Meel GJ, Keunen JE, van Norren D. Mizuo phenomenon
346 in X-linked retinoschisis. Pathogenesis of the Mizuo phenomenon. *Arch Ophthalmol*
347 1991;109:1104-1108.

348 11. Kuroda M, Hiram Y, Nishida A, et al. [A case of Oguchi disease with disappearance
349 of golden tapetal-like fundus reflex after vitreous resection]. *Nihon Ganka Gakkai Zasshi*
350 2011;115:916-923.

351 12. Usui T, Ichibe M, Ueki S, et al. Mizuo phenomenon observed by scanning laser
352 ophthalmoscopy in a patient with Oguchi disease. *Am J Ophthalmol* 2000;130:359-361.

353 13. Yamada K, Motomura Y, Matsumoto CS, Shinoda K, Nakatsuka K. Optical
354 coherence tomographic evaluation of the outer retinal architecture in Oguchi disease.
355 *Jpn J Ophthalmol* 2009;53:449-451.

- 356 14. Takada M, Otani A, Ogino K, Yoshimura N. Spectral-domain optical coherence
357 tomography findings in the Mizuo-Nakamura phenomenon of Oguchi disease. *Retina*
358 2011;31:626-628.
- 359 15. Godara P, Cooper RF, Sergouniotis PI, et al. Assessing retinal structure in complete
360 congenital stationary night blindness and Oguchi disease. *Am J Ophthalmol*
361 2012;154:987-1001 e1001.
- 362 16. Sergouniotis PI, Davidson AE, Sehmi K, Webster AR, Robson AG, Moore AT.
363 Mizuo-Nakamura phenomenon in Oguchi disease due to a homozygous nonsense
364 mutation in the SAG gene. *Eye (London, England)* 2011;25:1098-1101.
- 365 17. Sato T, Baba K. Appearance and disappearance of the fundus disturbance in
366 Oguchi's disease. *Am J Ophthalmol* 1961;51:243-248.
- 367 18. Hogan MJ, Feeney L. THE ULTRASTRUCTURE OF THE RETINAL BLOOD
368 VESSELS. I. THE LARGE VESSELS. *Journal of ultrastructure research* 1963;39:10-28.
- 369 19. Heckenlively JR, Weleber RG. X-linked recessive cone dystrophy with tapetal-like
370 sheen. A newly recognized entity with Mizuo-Nakamura phenomenon. *Arch Ophthalmol*
371 1986;104:1322-1328.
- 372 20. Robson AG, Mengher LS, Tan MH, Moore AT. An unusual fundus phenotype of inner
373 retinal sheen in X-linked retinoschisis. *Eye (London, England)* 2009;23:1876-1878.

374 21. Falls HF, Cotterman CW. Choroidoretinal degeneration: A sex-linked form in which
375 heterozygous women exhibit a tapetal-like retinal reflex. *Archives of Ophthalmology*
376 1948;40:685-703.

377 **Figure legends**

378

379 **Figure 1.** Fundus photographs of eyes with Oguchi's disease showing clearly
380 demarcated dark regions. The dark regions without tapetal-like reflexes are located
381 along or posterior to the equator (arrows) in Case 1 (**A and B**), Case 2 (**C and D**), Case
382 3 (**E**) and Case 11 (**F**).

383

384 **Figure 2.** Dark regions demarcated by retinal arteries. The locations of the retinal
385 arteries are shown by white dots in the right columns. The dark regions are partially
386 demarcated by retinal arteries but not by veins (arrows), in the right eye of Case 1 (**A**),
387 the left eye of Case 1 (**B**), the left eye of Case 2 (**C**), and the left eye of Case 3 (**D**).

388

389 **Figure 3.** Optical coherence tomographic (OCT) image (**A**) and fundus
390 autofluorescence (AF) image (**B**) of a case with clearly demarcated dark regions.
391 Horizontal scan image was obtained for 9.0 mm in the superior-temporal portion of the
392 right eye in Case 1 across the regions with and without tapetal-like reflex (**A, right**).
393 The border between the dark region and the region with the tapetal-like reflex in the OCT
394 image is indicated by an arrow. The reflectance of the photoreceptor layer is much

395 higher in the region with tapetal-like reflex than in the dark region. There are no
396 apparent structural abnormalities in either the inner retinal layers or outer retinal layers or
397 the choroid. In the AF image, there are no demarcated lesions corresponding to the
398 dark regions in the fundus photograph (**B, asterisks**).

399

400 **Figure 4.** Expansion and contraction of the dark regions during the follow-up period.

401 The area of the dark region is reduced and the tapetal-like reflex expanded during the 4
402 year and 5 months follow-up in the superior portion of the right eye of Case 1 (**A**). The
403 dark region is reduced and absent during the 4 year and 7 months follow-up in the left
404 eye of case 2 (**B**). The dark region expanded during 2 years and 2 months follow-up in
405 the right eye of Case 3 (**C**). The regions with and without tapetal-like reflex interlaced,
406 and the dark region either expanded or contracted during the follow-up period depending
407 on the retinal locations in the right eye of Case 1 (**D**). Photographs of individual patients
408 were aligned so that their vertical retinal locations matched the others. The borders
409 between the dark regions and the regions with tapetal-like reflex at the different ages of
410 examination are indicated by either white dots or black dots or asterisks.

411

412 **Figure 5.** Comparison of the borders of the dark regions during light-adaptation.

413 Prolonged dark-adaptation for 180 minutes reduced the area of the tapetal-like reflex
414 (Mizuo-Nakamura phenomenon) in the right eye of Case 1 (**A, left**). After 20 minutes of
415 light-adaptation, the tapetal-like reflex reappeared (**A, right**). In the magnified image of
416 the superior retina (**B**), the dark region became clearly visible at the same location and
417 its border did not change during the course of light-adaptation (**white arrows**).
418 DA; dark-adaptation, LA; light-adaptation. Arrows indicate the same retinal locations in
419 the superior retina.

420

421 **Figure 6.** High and low reflective regions along the peripheral arteries.

422 (**A**) Highly reflective regions are observed along the retinal arteries (**arrowheads**) but
423 not along the veins.

424 (**B**) Low reflective regions are observed along the retinal arteries (**arrowheads**) but not
425 along the veins.

426 (**C**) Both high- and low-reflectivity regions are observed at the same location of the
427 retinal artery in the left eye of Case 4 (**C, left**). The dark regions are observed along
428 peripheral arteries, but located slightly apart from the vessels in the left eye (**C, middle**)
429 and right eye (**C, right**) of Case 3.

430 A; artery, V; vein.

431

432 **Figure 7.** A dark region running along the retinal nerve fiber layer (RNFL) bundle can
433 be seen in the nasal sector of the left eye of Case 4 (left). Prolonged dark-adaptation
434 for 180 minutes reduced the tapetal-like reflex, and the border of dark region cannot be
435 detected (middle). The dark region along the bundle of RNFL disappeared during the 3
436 years and 6 months of follow-up (right).
437 LA; light adaptation, DA; dark adaptation. Arrows indicate the same retinal locations in
438 the nasal retina.

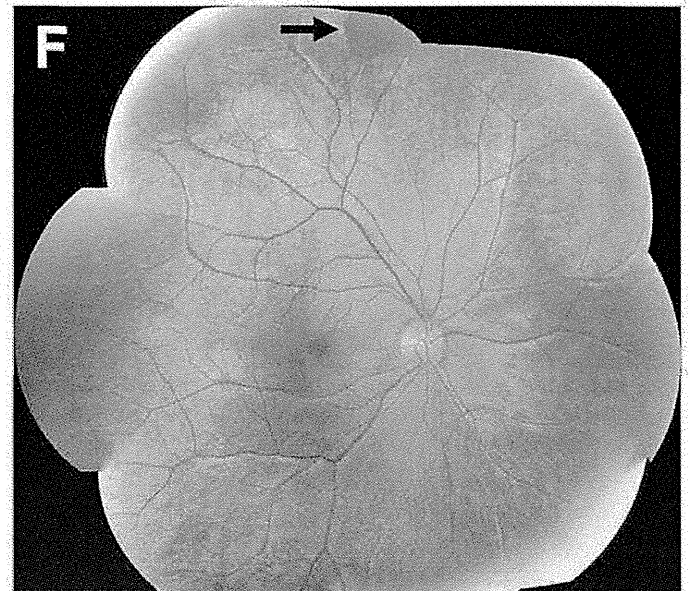
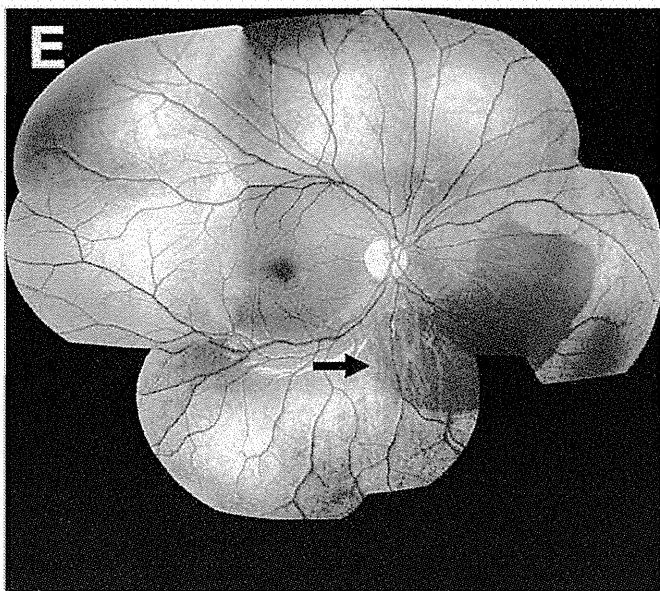
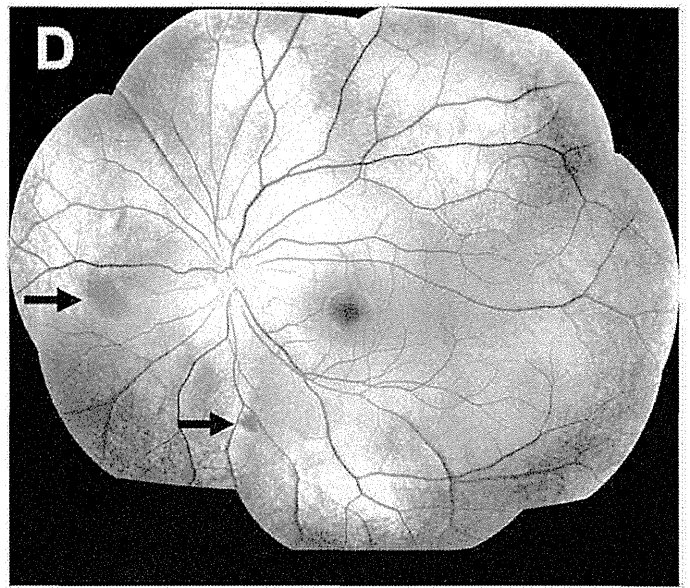
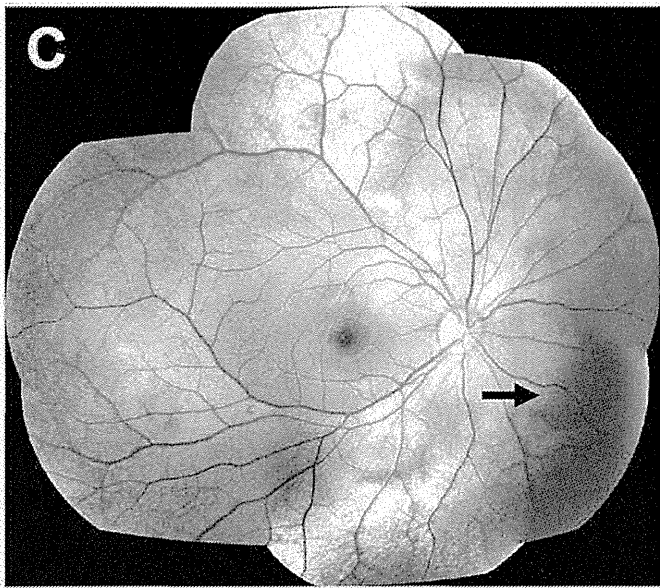
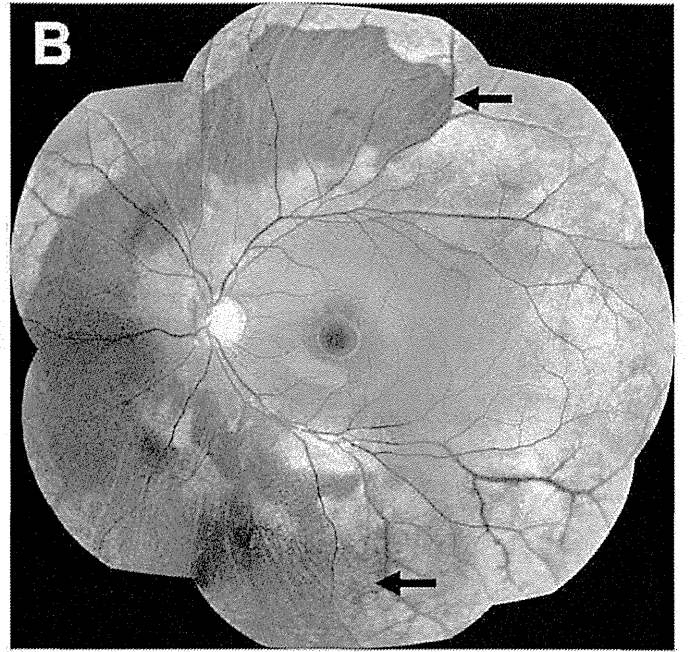
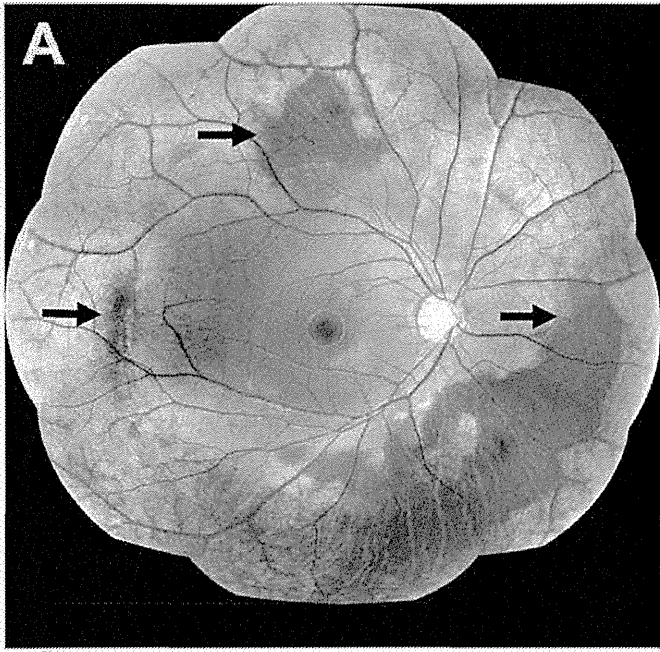
439

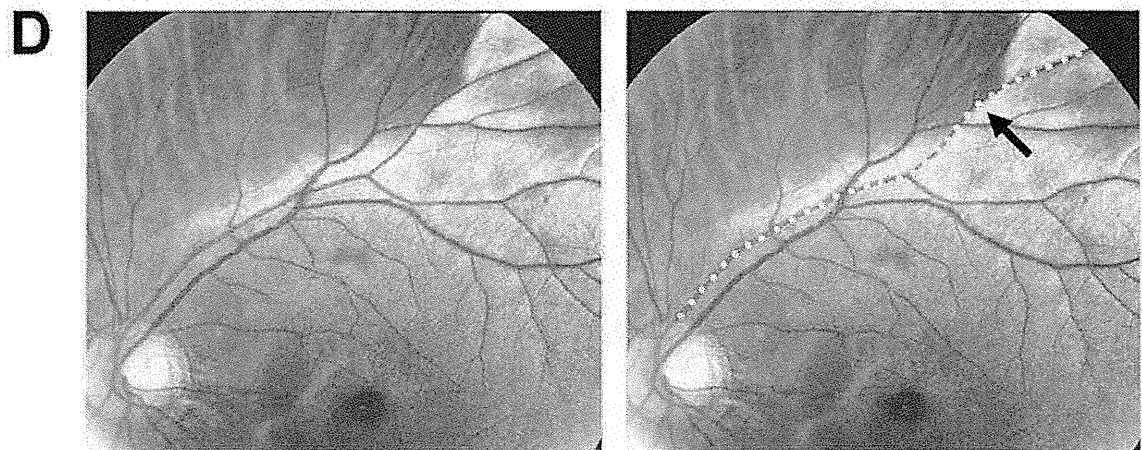
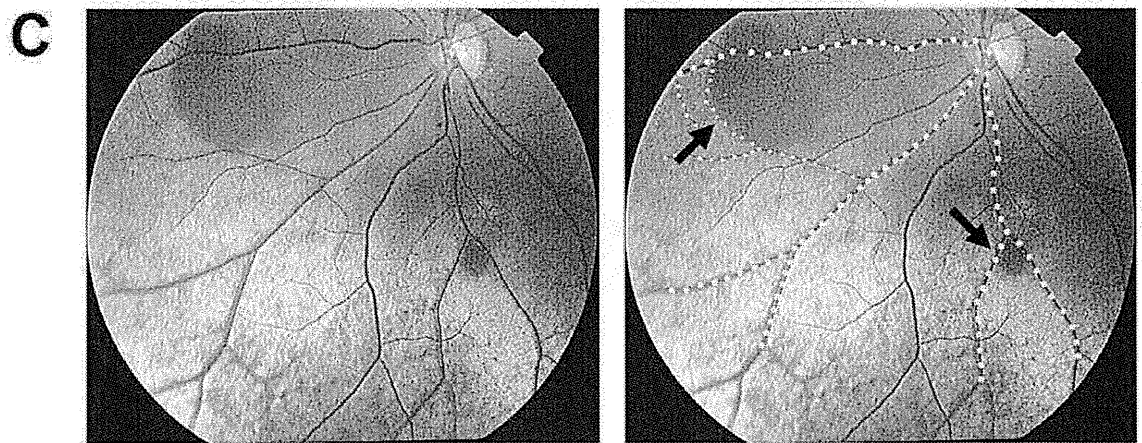
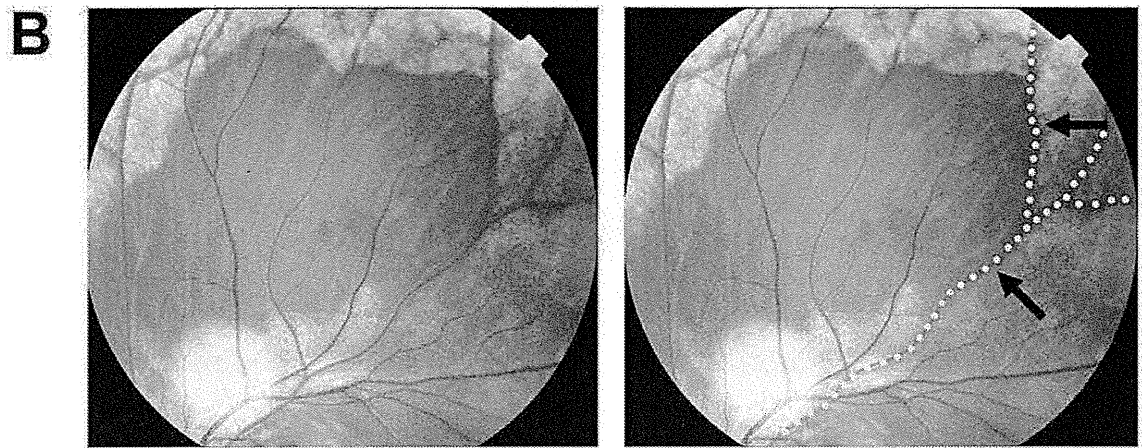
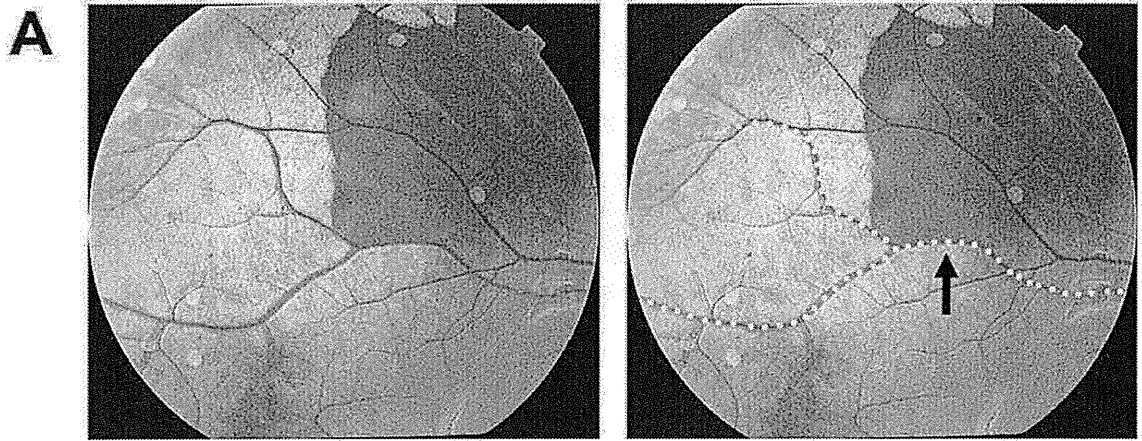
440 **Figure 8.** Optical coherence tomographic (OCT) images across the regions with and
441 without tapetal-like reflex. High-contrast vitreous images were obtained by a
442 swept-source OCT. Horizontal line scan images in the superior portion of the right (A)
443 and left (B) eyes in Case 1 are presented. The vitreous appears homogeneously
444 distributed over the dark regions, and a posterior vitreous detachment cannot be
445 observed. There were no abnormalities in the vitreoretinal interface along the border of
446 the dark regions (**arrows**).

447 **Acknowledgements**

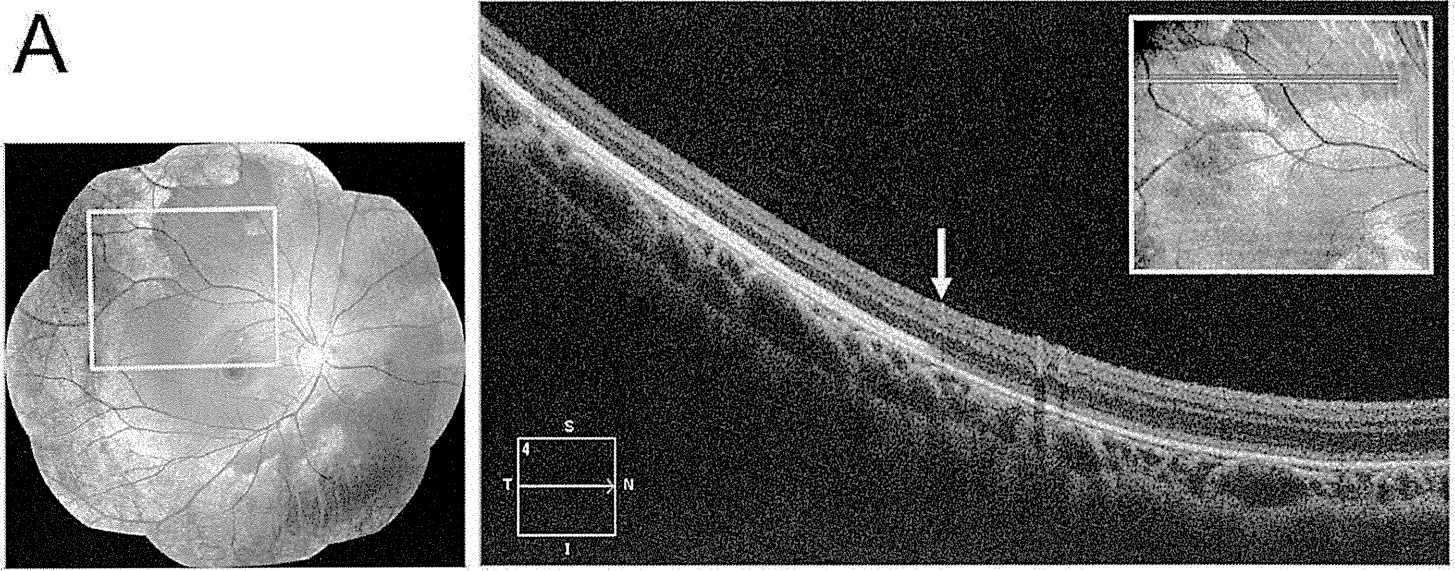
448 This research was supported by 1) research grants from the Ministry of Health, Labor
449 and Welfare, Japan and 2) Grant-in-Aid for Scientific Research, Japan Society for the
450 Promotion of Science, Japan. The authors have no financial conflict of interest.

451

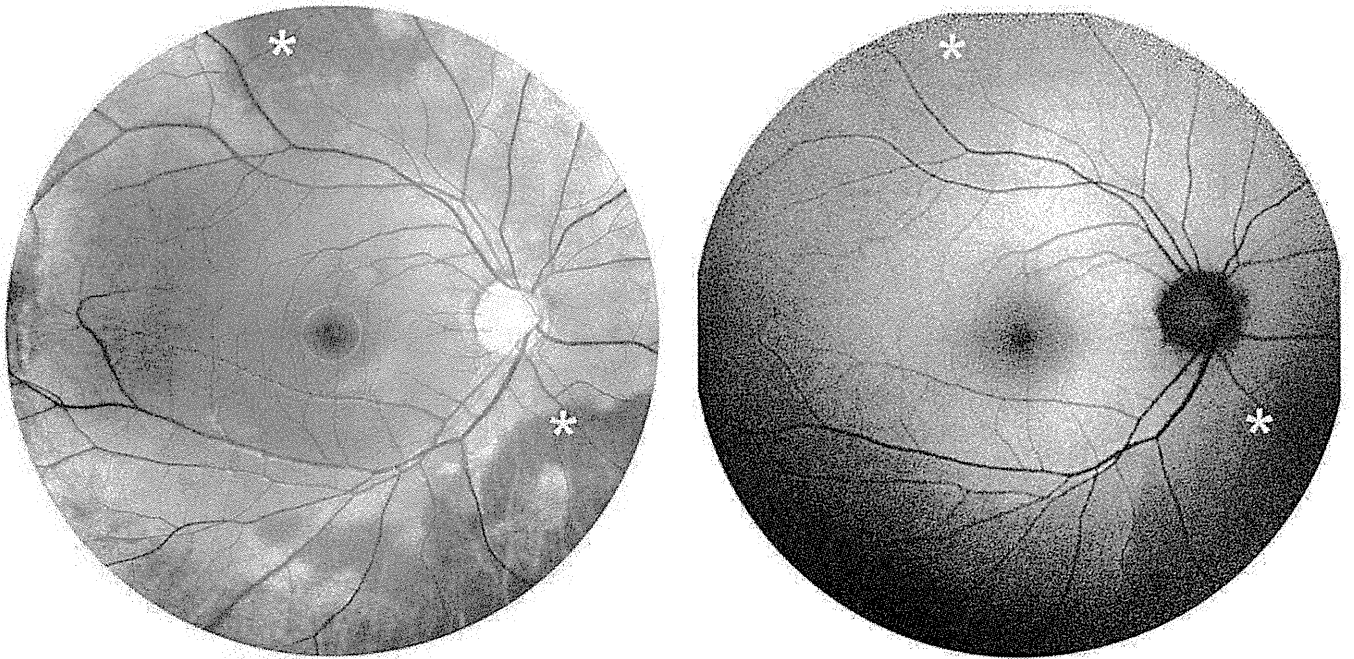


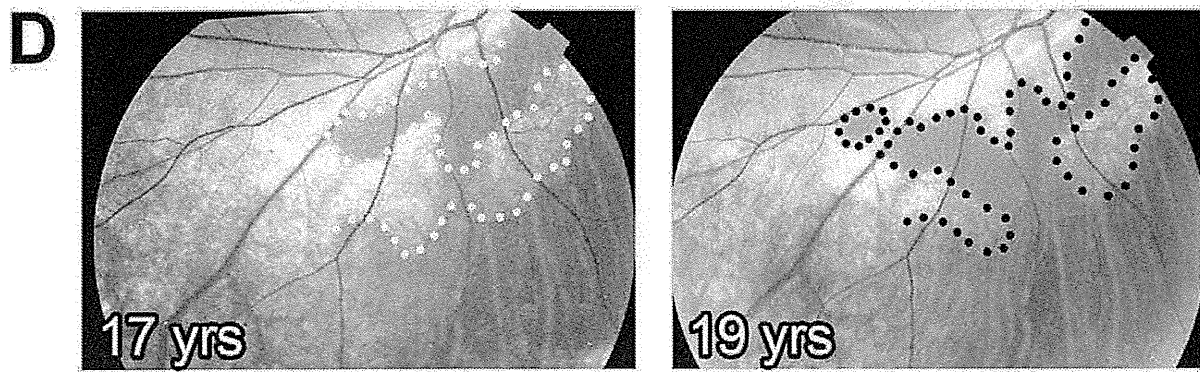
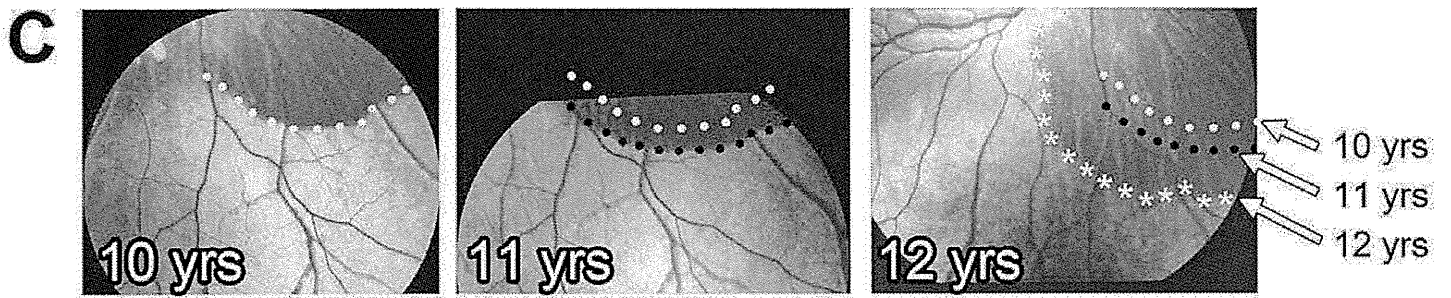
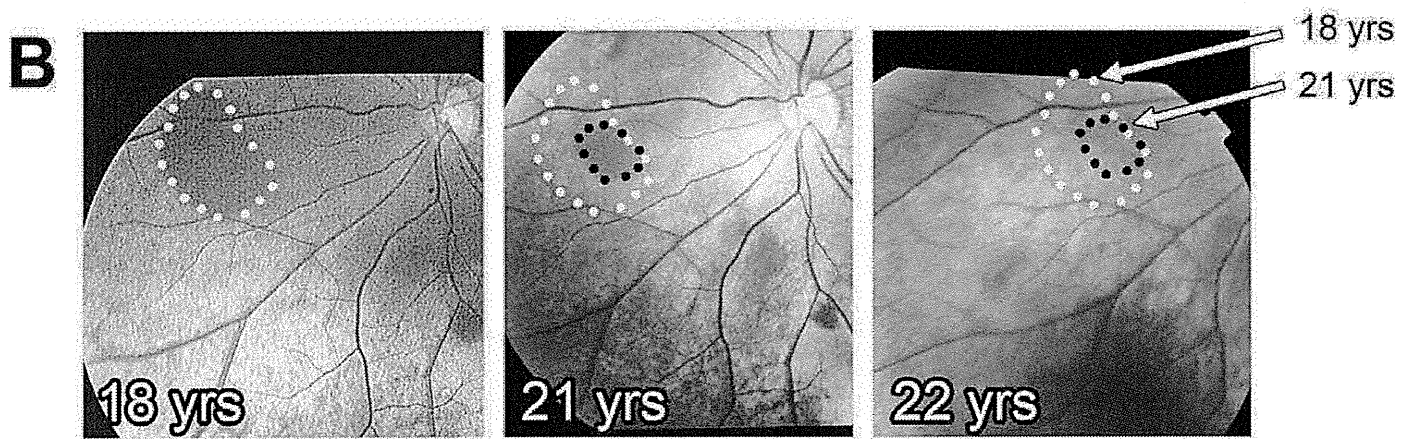
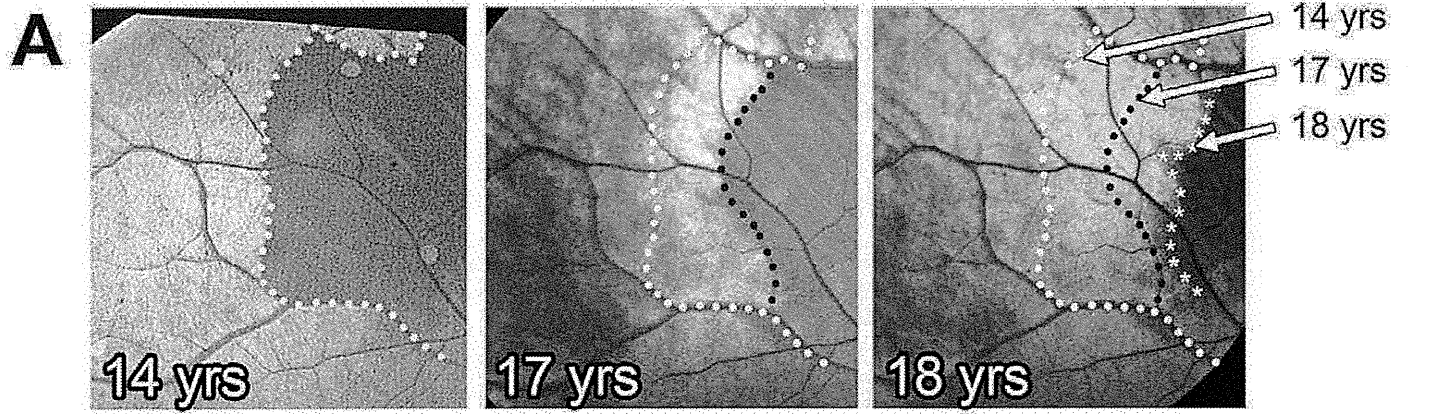


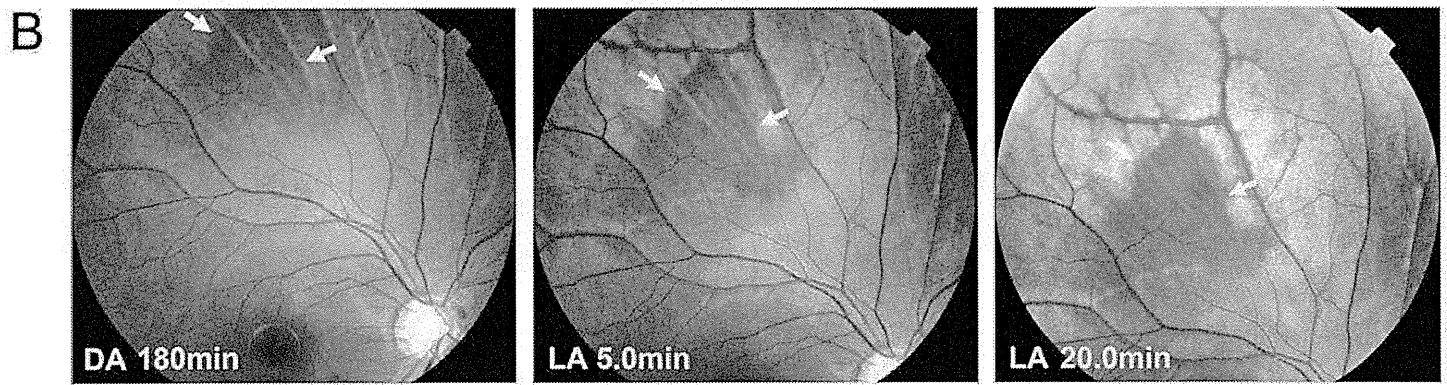
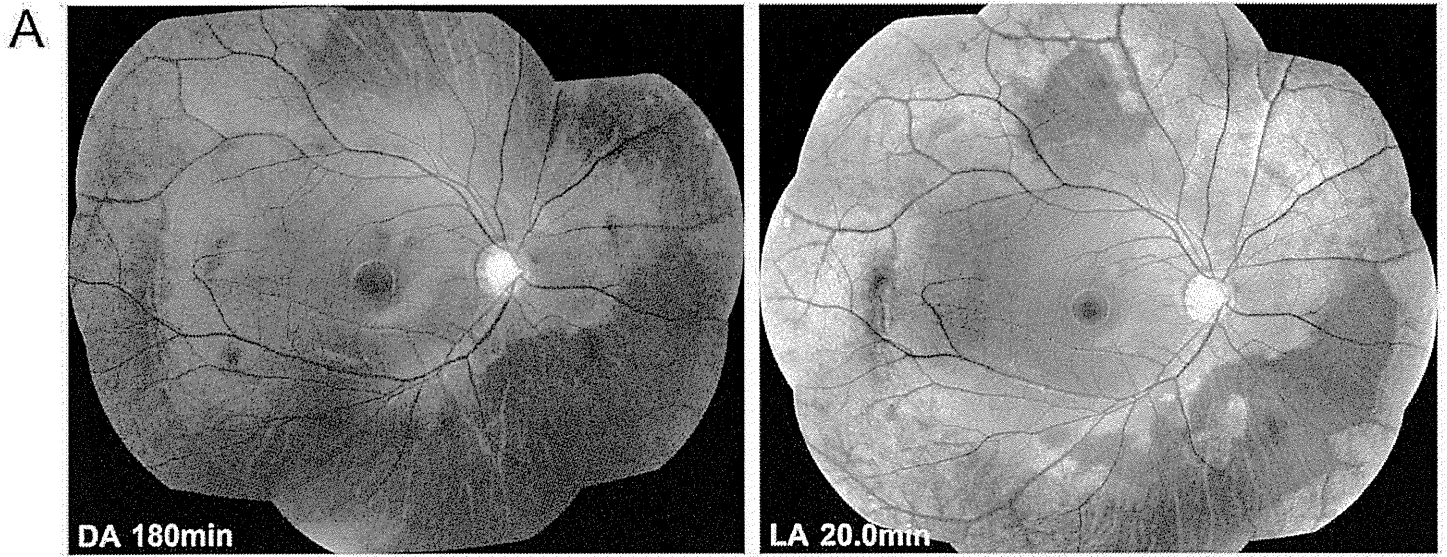
A

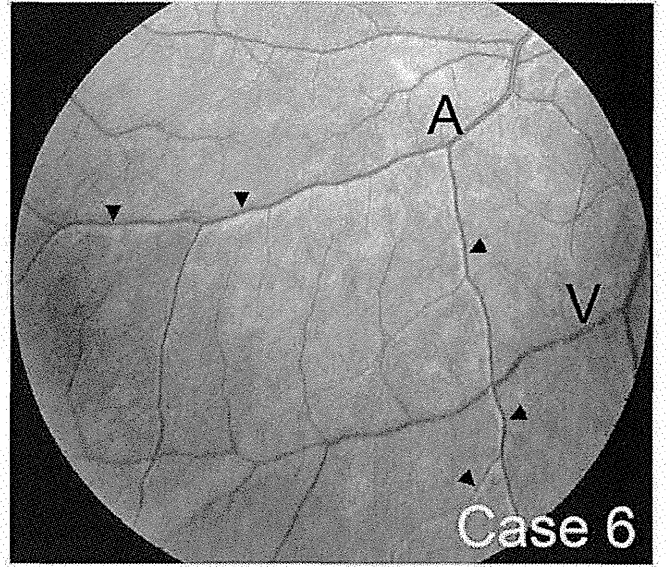
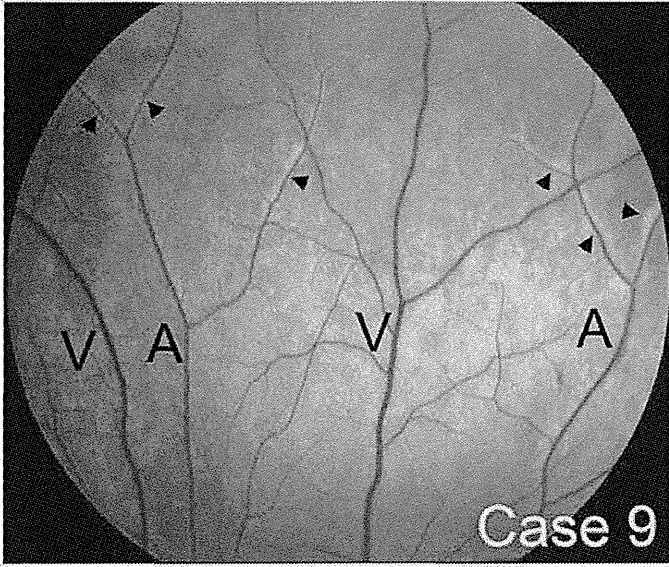
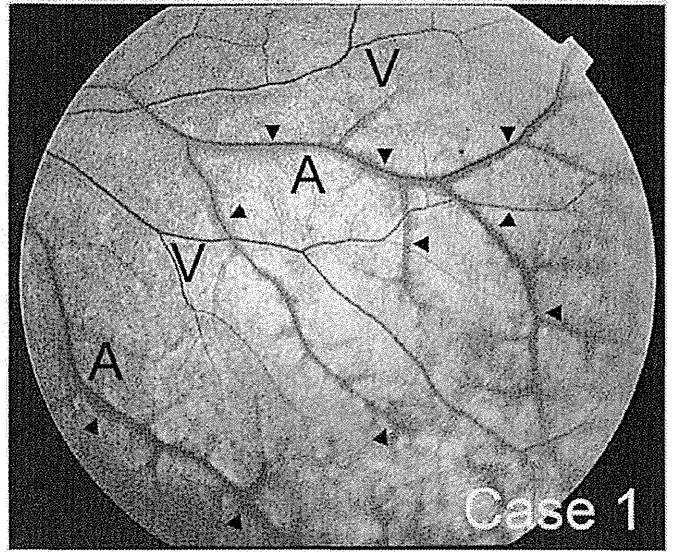
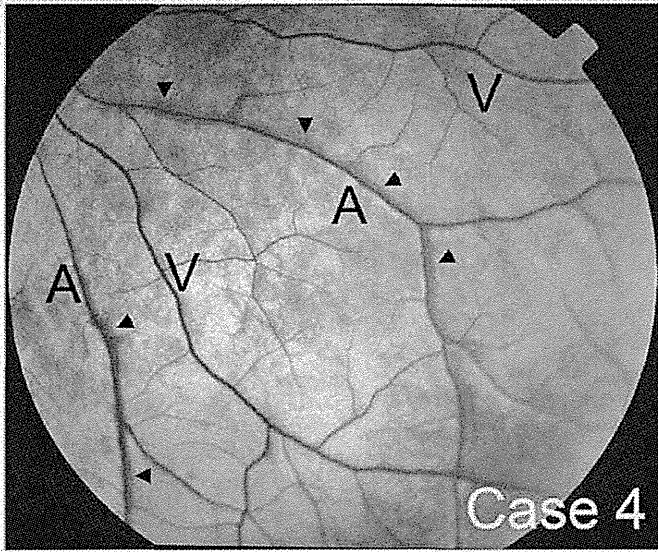
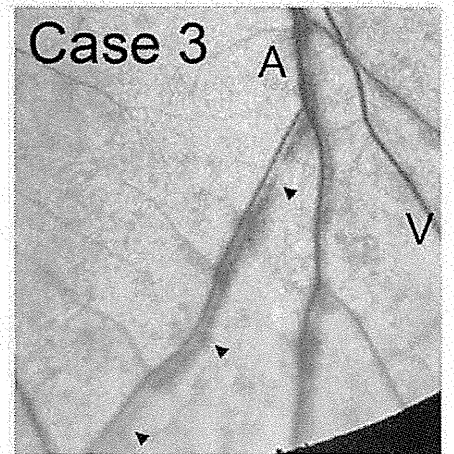
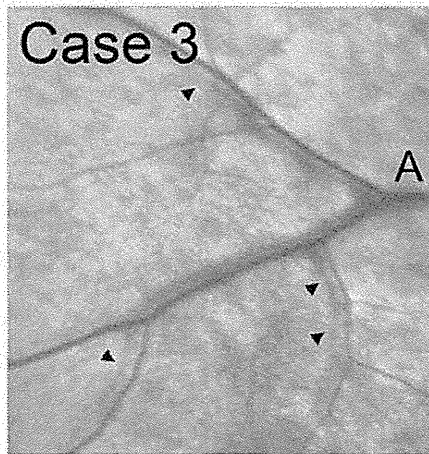
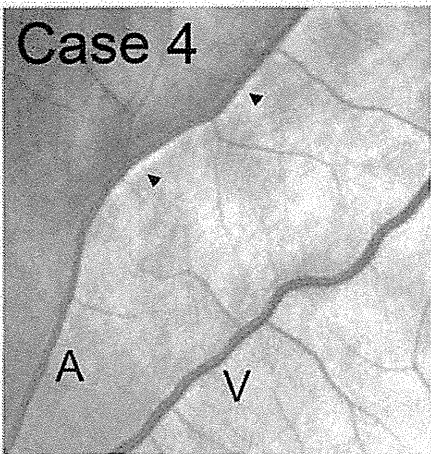


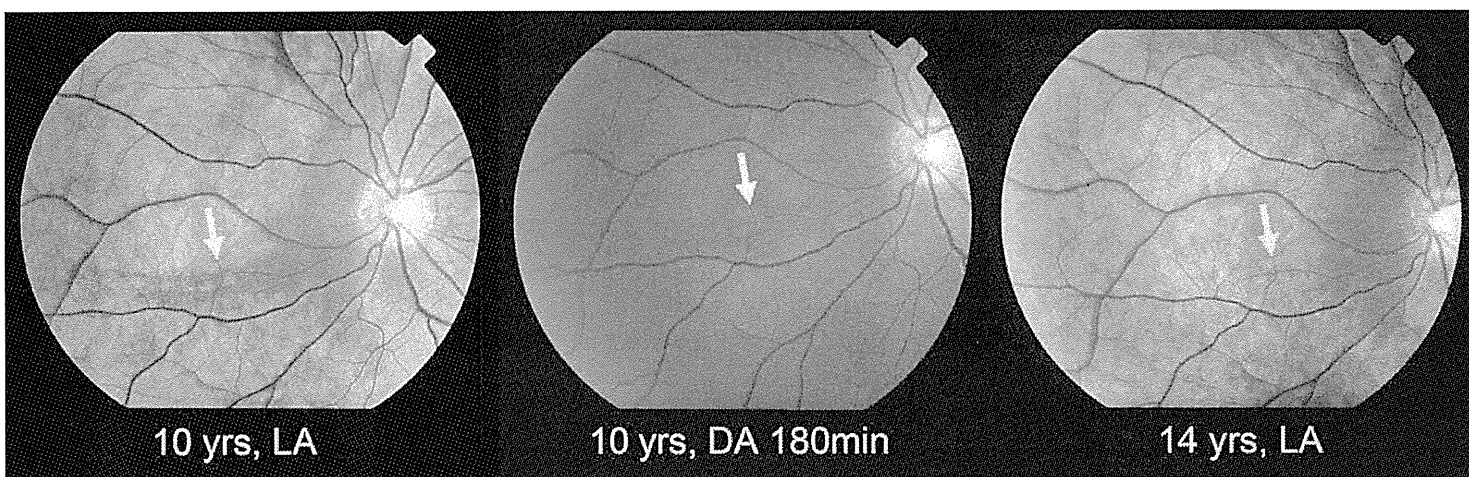
B







A**B****C**



10 yrs, LA

10 yrs, DA 180min

14 yrs, LA

